Bistatic Ultrasound Tomography

Todd Quinto
This includes joint work with
Gaik Ambartsoumian, Venky Krishnan, and Howard Levinson

Department of Mathematics
Tufts University
http://www.tufts.edu/~equinto

Geometric Analysis on Euclidean and Homogeneous Spaces, Tufts University
January 9, 2012

(Partial support from U.S. NSF)

Ultrasound Reflection Tomography (URT)

Acoustic waves are emitted from a source and reflect off of inhomogeneities inside the body. Their echoes are measured by a receiver. Then, emitter and receiver are moved about the body.

Ultrasound Reflection Tomography (URT)

Acoustic waves are emitted from a source and reflect off of inhomogeneities inside the body. Their echoes are measured by a receiver. Then, emitter and receiver are moved about the body.

This measured data are then used to reconstruct the unknown ultrasonic reflectivity function, which is used to generate cross-sectional images of the body.

Advantage:

- URT is safe and cost effective.
- URT does a good job imaging soft tissue.

Bistatic Data Acquisition Method

The ultrasound emitter is focussed to send sound waves in a plane.

- The emitter and receiver are separated on the circle, a fixed distance apart.
- The emitter and receiver rotate around the body on the circle (c =constant speed of sound, t =time).

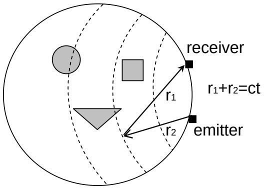

Separated emitted and receiver

Bistatic Data Acquisition Method

The ultrasound emitter is focussed to send sound waves in a plane.

- The emitter and receiver are separated on the circle, a fixed distance apart.
- The emitter and receiver rotate around the body on the circle ($c =$constant speed of sound, $t =$time).
- The data can be modeled as integrals of the reflectivity over ellipses with foci the emitter and receiver.

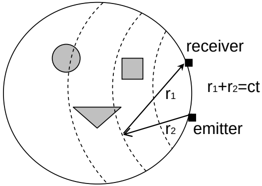

Separated emitted and receiver

Figure: A sketch of ellipses of integration in bistatic URT

The Parameters

The emitter and receiver move along the unit circle and are 2α radians apart, $\alpha \in (0, \pi/2)$.

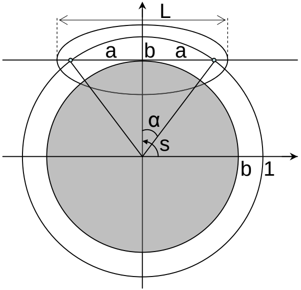

Figure: a, b, and D_b

$a = \sin(\alpha)$,

$b = \cos(\alpha)$

$2a =$distance between the foci

$D_b = \{x \in \mathbb{R}^2 \,|\, \|x\| < b\}$

The Parameters

The emitter and receiver move along the unit circle and are 2α radians apart, $\alpha \in (0, \pi/2)$.

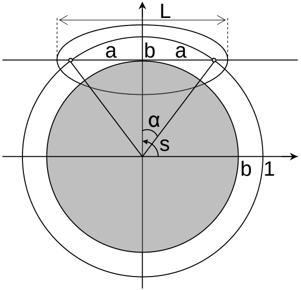

Figure: a, b, and D_b

$a = \sin(\alpha)$,

$b = \cos(\alpha)$

$2a =$distance between the foci

$$D_b = \{x \in \mathbb{R}^2 \,\big|\, \|x\| < b\}$$

For $s \in [0, 2\pi]$,
$\gamma_E(s) = (\cos(s-\alpha), \sin(s-\alpha))$
$\gamma_R(s) = (\cos(s+\alpha), \sin(s+\alpha))$

Ellipse: $E(s, L) = \{x \in \mathbb{R}^2 \,|\, \|x - \gamma_E(s)\| + \|x - \gamma_R(s)\| = L\}$

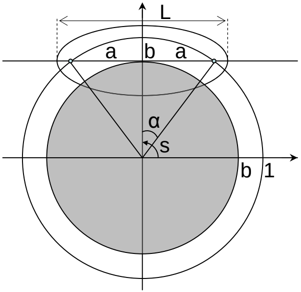

Figure: An ellipse $E(s, L)$

L is the major diameter–the sum of the distances from the foci to any point on the ellipse.

$s =$angle from the positive x axis to the center of the ellipse

The set of ellipses: $Y = \{(s, L) \,|\, s \in [0, 2\pi],\ L > 2a\}$

The Transforms

The Elliptical Radon Transform: $f \in \mathcal{E}'(D_b)$, $(s, L) \in Y$

$$\mathcal{R}f(s, L) = \int_{E(s,L)} f(x)dx$$

The Backprojection Transform: $g \in \mathcal{D}'(Y)$, $x \in D_b$

$$\mathcal{R}^*g(x) = \int_{s\in[0,2\pi]} g(s, \|x - \gamma_E(s)\| + \|x - \gamma_R(s)\|)ds$$

ds is standard Lebesgue measure and $\mathcal{R}^*$ is close to the L^2 adjoint of $\mathcal{R}$.
$\mathcal{R}^*$ is an integral of g over all ellipses through x.

Our Reconstruction Algorithm

For $f \in \mathcal{E}'(D_b)$, $\quad \mathcal{L}(f)(x) := \mathcal{R}^*(D\mathcal{R}f)(x)$
where D is a second order differential operator to be chosen using microlocal analysis.

This is a generalization of Lambda tomography for the line transform: $R^*(-d^2/dp^2)Rf = \sqrt{-\Delta}f$.

Our Reconstruction Algorithm

For $f \in \mathcal{E}'(D_b)$, $\quad \mathcal{L}(f)(x) := \mathcal{R}^*(D\mathcal{R}f)(x)$
where D is a second order differential operator to be chosen using microlocal analysis.

This is a generalization of Lambda tomography for the line transform: $R^*(-d^2/dp^2)Rf = \sqrt{-\Delta}f$.

We have developed derivative-backprojection algorithms

- SPECT [Bakhos, Chung, Q]
- Electron Microscopy [Q, Öktem]
- Common Offset Bistatic Synthetic Aperture Radar [Levinson, Q]
- Sonar [Q, Rieder, Schuster]

Our Reconstruction Algorithm and Microlocal Analysis

For $f \in \mathcal{E}'(D_b)$, $\quad \mathcal{L}(f)(x) := \mathcal{R}^*(D\mathcal{R}f)(x)$
where D is a second order differential operator to be chosen using microlocal analysis.

This is a generalization of Lambda tomography for the line transform: $R^*(-d^2/dp^2)Rf = \sqrt{-\Delta}f$.

We have developed derivative-backprojection algorithms and analyzed their microlocal properties

- SPECT [Bakhos, Chung, Q] Admissible Line Transform
- Electron Microscopy [Q, Öktem] Admissible Line Transform
- Common Offset Bistatic Synthetic Aperture Radar [Levinson, Q] Like an Elliptical Transform
- Sonar [Q, Rieder, Schuster] Spherical Transform

In each case the forward operator is a FIO related to a Radon transform.

Double Fibration and FIO

Incidence Relation: $Z = \{(s, L; x) \in Y \times D_b \big| x \in E(s, L)\}$.

Guillemin used the double fibration

$$\begin{tikzcd} & Z \arrow[dl, "\pi_L"'] \arrow[dr, "\pi_R"] & \\ Y & & D_b \end{tikzcd}$$

to prove microlocal properties of generalized Radon transforms.

[Ambartsoumian, Krishnan, Q] prove that $\mathcal{R}$ fits into Guillemin's theory since both projections are fiber maps and π_R has compact fiber, S^1.

Guillemin [G 1975, GS, G 1985] showed that generalized Radon transforms defined by such double fibrations are elliptic FIOs. The canonical relation is $\mathcal{C} = (N^*(Z) \setminus \mathbf{0})'$:

$$
\begin{array}{ccc}
 & \mathcal{C} & \\
\Pi_L \swarrow & & \searrow \Pi_R \\
T^*(Y) & & T^*(X)
\end{array}
$$

The Main Theorem

Guillemin [G 1975, GS, G 1985] showed that generalized Radon transforms defined by such double fibrations are elliptic FIOs. The canonical relation is $\mathcal{C} = (N^*(Z) \setminus \mathbf{0})'$:

$$\begin{array}{ccccc} & & \mathcal{C} & & \\ & \stackrel{\Pi_L}{\swarrow} & & \searrow^{\Pi_R} & \\ T^*(Y) & & & & T^*(X) \end{array}$$

Theorem (Ambartsoumian, Krishnan, Q)

For functions supported in D_b, $\mathcal{R}$ satisfies the Bolker Assumption: $\Pi_L : \mathcal{C} \to T^*(Y)$ is an injective immersion. Therefore, if D is elliptic, then our reconstruction operator $\mathcal{L} = \mathcal{R}^* D\mathcal{R}$ is an elliptic pseudodifferential operator from $\mathcal{E}'(D_b)$ to $\mathcal{D}'(D_b)$.

Notes

- The composition of two FIOs does not have to be a FIO, and many FIO do not satisfy the Bolker assumption: our transform in D_b is special.
- Our theorem implies that, for $f \in \mathcal{E}'(D_b)$, $\mathcal{L}(f)$ shows all singularities of f in D_b.

Notes

- The composition of two FIOs does not have to be a FIO, and many FIO do not satisfy the Bolker assumption: our transform in D_b is special.
- Our theorem implies that, for $f \in \mathcal{E}'(D_b)$, $\mathcal{L}(f)$ shows all singularities of f in D_b.
- If one considers a larger domain than D_b, then $\mathcal{R}$ does not fit into this framework since π_R is no longer proper, and the fibers are not closed manifolds. Π_L drops rank and singularities can be added to the reconstruction.

Notes

- The composition of two FIOs does not have to be a FIO, and many FIO do not satisfy the Bolker assumption: our transform in D_b is special.
- Our theorem implies that, for $f \in \mathcal{E}'(D_b)$, $\mathcal{L}(f)$ shows all singularities of f in D_b.
- If one considers a larger domain than D_b, then $\mathcal{R}$ does not fit into this framework since π_R is no longer proper, and the fibers are not closed manifolds. Π_L drops rank and singularities can be added to the reconstruction.
- In the proof, we put coordinates on $\mathcal{C}$, (s, L, ϕ, η) where ϕ is a "polar angle" on the ellipse $E(s, L)$ and $\eta \in \mathbb{R} \setminus 0$ is a cotangent coordinate. We reduce to proving that, as a function of ϕ, Π_L is an injective immersion.

Reconstructions

My senior honors thesis student Howard Levinson implemented the algorithm and showed that $D = -d^2/dL^2$ gives better reconstructions than $-d^2/ds^2$ (for microlocal reasons!).

Reconstructions

My senior honors thesis student Howard Levinson implemented the algorithm and showed that $D = -d^2/dL^2$ gives better reconstructions than $-d^2/ds^2$ (for microlocal reasons!).

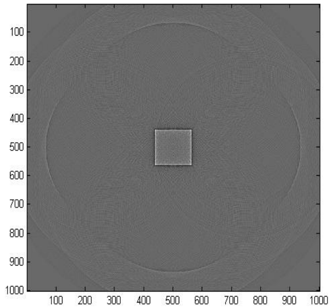

Figure: Reconstruction of a square

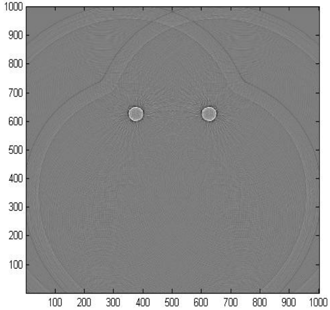

Figure: Reconstruction of two circles

Reconstructions

My senior honors thesis student Howard Levinson implemented the algorithm and showed that $D = -d^2/dL^2$ gives better reconstructions than $-d^2/ds^2$ (for microlocal reasons!).

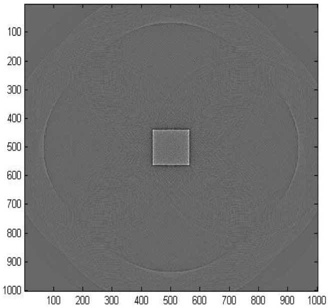

Figure: Reconstruction of a square

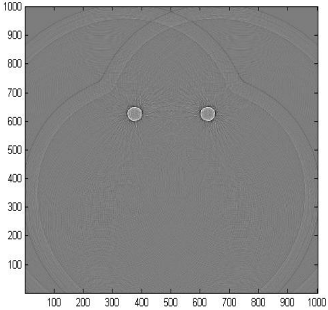

Figure: Reconstruction of two circles

Artifacts are outside of D_b!